

# Thiazolidinediones Increase Plasma-Adipose Tissue FFA Exchange Capacity and Enhance Insulin-Mediated Control of Systemic FFA Availability

Nicholas D. Oakes, Pia G. Thalén, Severina M. Jacinto, and Bengt Ljung

We studied the effects of thiazolidinedione treatment (rosiglitazone 1 or 10  $\mu\text{mol} \cdot \text{kg}^{-1} \cdot \text{day}^{-1}$  or darglitazone 1.3  $\mu\text{mol} \cdot \text{kg}^{-1} \cdot \text{day}^{-1}$  for 3 weeks) on lipid metabolism in obese Zucker rats. In the basal 7-h fasted state, rosiglitazone (10  $\mu\text{mol} \cdot \text{kg}^{-1} \cdot \text{day}^{-1}$ ) and darglitazone corrected the hypertriglyceridemia by increasing plasma triglyceride (TG) clearance and decreasing hepatic TG production, as assessed using Triton WR 1339. Free fatty acid (FFA) metabolism was assessed using  $^3\text{H}$ -palmitate tracer by estimating rates of plasma FFA appearance ( $R_a$ ), whole-body FFA oxidation ( $R_{ox}$ ), and tissue-specific nonoxidative FFA disposal ( $R_{fs}$ ). Basal  $R_a$ , plasma FFA levels, and clearance were increased by both thiazolidinediones. Detailed studies were conducted with darglitazone, which under basal conditions increased  $R_a$  (+114%),  $R_{ox}$  (+51%), and  $R_{fs}$  in adipose tissues. During euglycemic clamps performed at insulin levels corresponding to those observed postprandially, darglitazone increased the glucose infusion rate from 4.7 to 13.3  $\text{mg} \cdot \text{min}^{-1}$  and, in contrast to the basal state, it decreased  $R_a$  (-67%),  $R_{ox}$  (-84%), and  $R_{fs}$  in adipose tissue, muscle, and liver. We concluded that thiazolidinediones 1) ameliorate hypertriglyceridemia by lowered hepatic TG production and augmented TG clearance (two separate kinetic effects), 2) enhance insulin-mediated suppression of systemic FFA mobilization while increasing the capacity to mobilize FFA during fasting, 3) increase FFA trafficking into adipose tissue by increasing the ability of adipose tissue to take up and store FFA, and 4) enhance metabolic flexibility by improving glucoregulation under hyperinsulinemic conditions (possibly involving reduced skeletal muscle and liver exposure to fatty acids) and augmenting the capacity to utilize FFAs during fasting. *Diabetes* 50: 1158–1165, 2001

From Integrative Pharmacology, AstraZeneca R&D Mölndal, Mölndal, Sweden.

Address correspondence and reprint requests to N.D. Oakes, AstraZeneca R&D Mölndal, S-431 83 Mölndal, Sweden. E-mail: Nick.Oakes@astrazeneca.com.

Received for publication 19 May 2000 and accepted in revised form 9 February 2001.

BAT, brown adipose tissue; DAR, rats treated with darglitazone; FFA, free fatty acid; GIR, glucose infusion rate; HGP, hepatic glucose production;  $K$ , rate of FFA clearance;  $K_p$ , clearance rate of  $^3\text{H}$ -P;  $K_{fs}$ , rate of FFA incorporation into storage products;  $K_{TG}$ , TG clearance rate; LN, lean controls; OB, obese controls; PPAR $\gamma$ , peroxisome proliferator-activated receptor  $\gamma$ ;  $R_a$ , rate of FFA appearance;  $R_{fs}$ , rate of nonoxidative FFA disposal;  $R_{ox}$ , rate of FFA oxidation; ROS, rats treated with rosiglitazone; HTGO, hepatic TG output; RQ, red quadriceps muscle; TG, triglyceride; WAT, inguinal adipose tissue; WQ, white quadriceps.

Thiazolidinediones are structurally related agents used for the treatment of type 2 diabetes. In addition to improving glucose metabolic insulin sensitivity and reducing the requirement for insulin, these agents impressively reduce hypertriglyceridemia and have been reported to lower plasma free fatty acid (FFA) levels in various animal models of insulin resistance (1–4). Despite the fact that these compounds have been studied for almost 20 years (5), the in vivo mechanisms of insulin-sensitization remain unclear. Improvements in glucoregulation may occur via their action on lipid metabolism; a body of evidence suggests that an oversupply of fatty acids to insulin-sensitive target tissues, particularly liver and skeletal muscle, contributes to the development of insulin resistance (6). Treatment-induced reductions in fatty acid availability may thus contribute to the insulin-sensitizing effects of these compounds.

Thiazolidinediones may exert their effects via ligand activation of peroxisome proliferator-activated receptor  $\gamma$  (PPAR $\gamma$ ) (7), which is expressed primarily in adipose tissue (8). PPAR $\gamma$  activation contributes to the triggering of differentiation of preadipocytes (9) and induces expression of genes involved in the transport and sequestration of FFA (10). These cellular and molecular effects of PPAR $\gamma$  agonism could influence FFA exchange between adipose and other tissues, but direct evidence based on measurements of in vivo fluxes and the metabolic fate of FFA are lacking.

We report here the effects of two thiazolidinediones, rosiglitazone and darglitazone, in obese insulin-resistant/dyslipidemic Zucker *fa/fa* rats. The aim was to elucidate effects on FFA and triglyceride metabolism. Because of the potentially central effect of altered FFA metabolism on the beneficial effects of thiazolidinediones, we undertook a detailed evaluation of in vivo FFA mobilization and metabolic fate using  $^3\text{H}$ -palmitate tracer methods. The results demonstrate extensive effects in adipose tissue; notably, there was an increased ability to take up and store plasma FFA, an augmented capacity to mobilize FFAs under fasting conditions, and a greatly enhanced ability of postprandial levels of insulin to suppress FFA mobilization. Investigation into the kinetic mechanisms of plasma triglyceride (TG) lowering showed that abolition of hypertriglyceridemia by thiazolidinediones involves both accelerated removal of TG from VLDL particles and decreased hepatic TG production.

## RESEARCH DESIGN AND METHODS

**Animals and general procedures.** Experimental procedures were approved by the Local Ethics Review Committee on Animal Experiments (Göteborg region). Male 8-week-old Zucker rats (Charles River Wiga GmbH, Suffield, Germany) were housed in a facility with controlled temperature (20–22°C) and humidity (40–60% RH) with a 12-h light-dark cycle (lights on 6:00 A.M.). The animals had free access to rodent diet (R3; Laktamin AB, Stockholm, Sweden) and tap water.

**Treatment groups.** Lean (*Fa/fa*) and obese (*fa/fa*) Zucker rats were studied in five groups: lean untreated controls (LN), obese untreated controls (OB), and obese treated with rosiglitazone 1  $\mu\text{mol} \cdot \text{kg}^{-1} \cdot \text{day}^{-1}$  (ROS1), rosiglitazone 10  $\mu\text{mol} \cdot \text{kg}^{-1} \cdot \text{day}^{-1}$  (ROS10), or darglitazone 1.3  $\mu\text{mol} \cdot \text{kg}^{-1} \cdot \text{day}^{-1}$  (DAR). Treated rats were dosed daily at 1:00 P.M. for 3 weeks by gastric gavage. Untreated control rats were gavaged with an equal volume of vehicle (0.5% carboxymethyl cellulose, 2.5 ml  $\cdot \text{kg}^{-1}$ ).

**Anesthetized rat preparation.** On the morning of the study, food was withdrawn at 7:00 A.M. Rats were anesthetized at 10:00 A.M. with Na-thiobutabarbital (Inactin; RBI, Natick, MA), with the lean and obese rats receiving 120 and 180  $\text{mg} \cdot \text{kg}^{-1}$ , respectively. Body temperature was monitored with a rectal probe and maintained between 37.5 and 38.0°C throughout the experiment. Animals were tracheotomized, and catheters were placed in the right jugular vein and left carotid artery. Arterial catheter patency was maintained throughout the experiment by continuous infusion (10  $\mu\text{l} \cdot \text{min}^{-1}$ ) of a sterile saline solution containing sodium citrate (20.6 mmol/l). Acute experimental protocols (see below) were commenced at 2:00 P.M. after a 1.5-h postsurgery stabilization period.

**Conscious, chronically catheterized rat preparation.** At 1 week before the acute study, rats were fitted with jugular and carotid catheters under isoflurane anesthesia. Prophylactic antibiotics were administered subcutaneously the day before surgery and on the day of the surgery (ampicillin 150  $\text{mg} \cdot \text{kg}^{-1}$ , Doktacillin; AstraZeneca). Cannulae were exteriorized via a small cutaneous incision at the nape of the neck, and patency was maintained before study by filling the lines with 45.5% (wt/wt) polyvinylpyrrolidone (molecular weight ~40,000) (Fluka Chemie AG, Buchs) dissolved in a 0.9% NaCl, 20.6 mmol/l sodium citrate solution. All rats included in the acute experiments were gaining weight and had recovered their preoperative body weights during the week after implantation. On the morning of the study, food was withdrawn at 7:00 A.M. After a 90-min posthookup settling-in period, the acute experiment was commenced at 2:00 P.M. in conscious unrestrained rats.

### Experimental protocols.

**Study 1: Hepatic VLDL triglyceride production and plasma clearance of triglyceride.** Five groups of anesthetized 7-h fasted rats were studied: LN, OB, ROS1, ROS10, and DAR. After a 90-min postsurgery stabilization period, basal arterial blood samples were collected. Rats then received an intravenous dose of 20% (wt/wt) Triton WR1339 (200  $\text{mg} \cdot \text{kg}^{-1}$  polymeric *p*-isooctylpolyoxyethylenephenol) (Tyloxapol; Sigma, St. Louis, MO) in normal saline. Arterial blood samples (0.2 ml) were collected 30, 60, 90, and 120 min after Triton administration. Plasma lipoprotein profiles (see below) were determined in a basal sample and a post-Triton (120 min) sample. Plasma TG determinations were made in all samples collected.

### Study 2: Mobilization and fate of plasma FFAs

**Tracer preparation.** Tracer infusates were freshly prepared each day. For every rat, 75  $\mu\text{l}$  ethanol containing  $\sim 2 \times 10^8$  dpm [ $9,10\text{-}^3\text{H}$ ]palmitic acid ( $^3\text{H-P}$ ; Amersham, Solna, Sweden) and 152 nmol Na-palmitate (Sigma) was added dropwise to 300  $\mu\text{l}$  of continuously stirred 4% (w/v) essentially fatty acid-free bovine serum albumin (Sigma) in normal saline. The infusate was increased to a final volume of  $\sim 3$  ml by the addition of normal saline.

**General tracer methodology.** The albumin-palmitate- $^3\text{H-P}$  complex was infused at a constant rate ( $\sim 1 \cdot 10^6$  dpm  $\cdot \text{min}^{-1}$ , 17  $\mu\text{l} \cdot \text{min}^{-1}$ ) into the jugular vein. To obtain plasma FFA and  $^3\text{H-P}$  concentrations, 150  $\mu\text{l}$  arterial blood samples were collected 10, 20, 40, 60, 80, 100, and 120 min after the start of tracer infusion. At 120 min, tracer infusion was stopped and additional blood samples were collected at 124, 128, 132, and 140 min. Plasma was rapidly separated in a refrigerated centrifuge, and a 25- $\mu\text{l}$  aliquot was placed directly into 2 ml lipid extraction mixture (described below). After collection of the 140-min blood sample, rats were given a lethal dose of Na-thiobutabarbital. Samples ( $\sim 100$  mg) of the following tissues were collected: red quadriceps muscle (RQ), white quadriceps (WQ), inguinal adipose tissue (WAT), interscapular brown adipose tissue (BAT), and liver. Tissue samples were weighed and placed in small cardboard cones for determination of  $^3\text{H}$  activity after combustion (see below).

**Whole-body FFA metabolism in anesthetized rats.** Five groups of anesthetized 7-h fasted Zucker rats were studied: LN, OB, ROS1, ROS10, and DAR. Experiments were performed to assess FFA metabolism only at the whole-body level and were thus performed according to the experimental procedure

detailed in the section above (*General tracer methodology*) until collection of the 120-min blood sample, at which time the experiment was terminated.

**Whole-body and tissue-specific FFA metabolism in conscious rats.** Two groups of conscious obese Zucker rats were studied: OB and DAR. Rats that were fasted for 7 h were studied in either the basal state or under conditions of the euglycemic-hyperinsulinemic glucose clamp. The tracer methodology described above was commenced in the basal studies after collection of the basal blood sample and in the clamp studies after establishing a glucose steady state ( $\sim 60$  min after starting the insulin infusion).

Clamp studies were performed at postprandial levels of hyperinsulinemia. Human insulin (Actrapid; Novo Nordisk A/S, Copenhagen) was infused via the jugular catheter using a syringe pump (Model 22 I/W; Harvard Apparatus, South Natick, MA). Arterial blood glucose was measured every 5 min using a glucose analyzer (YSI 2700; YSI, Yellow Springs, OH) and was clamped within 10% of the target level by manually adjusting a variable rate infusion of 30% (w/v) glucose in normal saline solution. Blood loss was minimized by a special direct sampling procedure from the arterial line (15  $\mu\text{l}/\text{sample}$ ). Glucose was infused with a syringe pump (CMA 1100; Carnegie Medicin, Solna, Sweden).

### Analysis of plasma and tissue samples.

**Plasma lipids, glucose, and insulin.** Colorimetric kit methods were used for the measurement of plasma FFA (NEFA C; Wako, Richmond, VA), triglycerides (Triglycerides/GB; Boehringer Mannheim, Indianapolis, IN), and glucose (Glucose HK; Roche, Stockholm). These methods were performed on a centrifugal analyzer (Cobas Bio; F. Hoffmann-La Roche & Co., Basle, Switzerland). Insulin concentrations were measured using radioimmunoassay (rat insulin RIA kit; Linco Research, St. Charles, MO).

**Resolution of plasma  $^3\text{H-P}$  and  $^3\text{H}_2\text{O}$ .** To discriminate  $^3\text{H-P}$  from total plasma  $^3\text{H}$  activity, a lipid extraction and separation procedure based on the method of Hagenfeldt (11) was performed on plasma samples. This involved an initial acid lipid extraction using a mixture of isopropanol-hexane-0.5 mol/l  $\text{H}_2\text{SO}_4$  (40:10:1) followed by a polarity separation step under alkaline conditions. This step partitioned neutral lipids (including esterified fatty acids) into a hexane phase, and it partitioned polar lipids (including  $^3\text{H-P}$ ) into an alcohol phase.  $^3\text{H}_2\text{O}$  was estimated as the  $^3\text{H}$  activity lost during evaporation of the lower (isopropanol-water) phase of the lipid extraction procedure.

**Measurement of tissue  $^3\text{H}$  activity.** Freshly collected tissue samples were desiccated in a freeze dryer to remove  $^3\text{H}_2\text{O}$ . Non- $^3\text{H}_2\text{O}$ -associated  $^3\text{H}$  activity was then determined using a Packard System 387 automated sample preparation unit (Packard Instrument, Meriden, CT), which completely oxidized the sample and collected the formed  $^3\text{H}_2\text{O}$  into scintillant (Monophase S; Packard Bioscience B.V., Groningen, The Netherlands) for counting.  $^3\text{H}$  activity was measured using liquid scintillation spectrometry (Wallac 1409 counter; Wallac OY, Turku, Finland).

**Lipoprotein profiles.** Cholesterol distribution profiles were measured in 10- $\mu\text{l}$  plasma samples by a size-exclusion high-performance liquid chromatography system using a Superose 6 PC 3.2/30 column (Amersham Pharmacia Biotech, Uppsala, Sweden), as previously described (12). For simplicity, the various peaks in the profiles are designated as VLDL, LDL, and HDL, analogous with the nomenclature used for the human profile.

**Liver triglyceride content.** Liver samples (40–50 mg) were extracted in 1 ml isopropanol. After centrifugation, 4- $\mu\text{l}$  aliquots of supernatant were added to 300  $\mu\text{l}$  reagent (Unimate 5 TRIG; F. Hoffman-La Roche AG, Basel) for enzymatic colorimetric determination of triglyceride concentration.

### Calculations.

**Study 1: Estimation of hepatic triglyceride output.** Triton WR1339 effectively blocks the clearance of plasma TG. When applied in the postabsorptive state, the rate of hepatic TG output (HTGO) can be calculated from the linear rate of accumulation of TG in plasma (13), assuming a lipoprotein distribution space of 4% of lean body mass. The plasma TG clearance rate ( $K_{TG}$ ), an index of the combined ability of the tissues to remove TG from the circulation, was calculated as the ratio of HTGO to  $C_{TG}$ , where  $C_{TG}$  refers to the basal plasma TG immediately before Triton administration.

### Study 2: Estimation of whole-body and tissue-specific rates of FFA metabolism.

**Rates of plasma FFA clearance and appearance.** Plasma FFA mobilization was assessed using a constant infusion of  $^3\text{H}$ -palmitate ( $^3\text{H-P}$ ). After attainment of isotopic steady states ( $< 40$  min after the start of tracer infusion), the plasma clearance rate of  $^3\text{H-P}$  ( $K_p$ ) was calculated as

$$K_p = i_p/c_p$$

where  $i_p$  is the tracer infusion rate (dpm  $\cdot \text{min}^{-1}$ ) and  $c_p$  is the steady state arterial concentration of  $^3\text{H-P}$  (dpm  $\cdot \text{ml}^{-1}$ ). The rate of appearance of plasma FFAs ( $R_a$ ) was calculated as

$$R_a = C_p \times K_p$$

where  $C_p$  is the arterial plasma FFA ( $\mu\text{mol} \cdot \text{ml}^{-1}$ ).

TABLE 1

Body weight and plasma factors in 3-h fasted lean control, obese control, and obese thiazolidinedione-treated conscious Zucker rats

	LN	OB	ROS1	ROS10	DAR
Pretreatment					
Body weight (g)	345 ± 8*	520 ± 15	499 ± 13	519 ± 16	532 ± 12
3-weeks treatment					
Body weight (g)	391 ± 8*	624 ± 15	664 ± 12†	708 ± 18*	745 ± 15*
Lean body mass (g)	317 ± 6*	368 ± 9	365 ± 7	411 ± 10‡	425 ± 8*
Fat body mass (g)	74 ± 2*	256 ± 6	299 ± 5*	297 ± 8*	320 ± 6*
Plasma glucose (mmol/l)	7.1 ± 0.1*	13.7 ± 1.0	9.5 ± 0.5*	7.8 ± 0.4*	9.4 ± 0.8*
Plasma insulin (nmol/l)	0.3 ± 0.02*	5.7 ± 0.4	3.0 ± 0.6*	0.88 ± 0.2*	0.64 ± 0.1*
Plasma TG (mmol/l)	1.5 ± 0.2*	8.9 ± 1.0	2.8 ± 0.6*	0.92 ± 0.1*	0.83 ± 0.1*

Results are expressed as means ± SE ( $n = 11-16$ ). \* $P < 0.001$ , † $P < 0.01$ , ‡ $P < 0.05$  versus OB.

*Rate of plasma FFA oxidation.* An estimate of the whole-body rate of FFA oxidation ( $R_{ox}$ ) was calculated from the plasma accumulation of  $^3\text{H}_2\text{O}$  as

$$R_{ox} = (c_w \times V_w / i_p \times T_{in}) \cdot R_a$$

where  $c_w$  is the plasma concentration of  $^3\text{H}_2\text{O}$  (at 140 min),  $V_w$  is the total water space of the rat (assumed to be 70% of lean body mass), and  $T_{in}$  is the tracer infusion time (120 min).

*Tissue-specific FFA metabolism.* Indexes of the tissue-specific clearance rates of plasma FFA incorporation into storage products ( $K_{fs}$ ) were calculated as

$$K_{fs} = m_p \int_0^T c_p(t) dt$$

where  $m_p$  is the tissue content of  $^3\text{H}$  activity associated with non- $^3\text{H}_2\text{O}$ -associated products of  $^3\text{H}$ -P (at  $t = T$ ),  $c_p$  is the arterial plasma concentration of  $^3\text{H}$ -P, and  $T$  is the time of tissue collection (140 min). Collection of tissues 20 min after infusion of  $^3\text{H}$ -P had stopped (see protocol above) ensured low plasma  $^3\text{H}$ -P at  $T$  and therefore minimal contribution of free unmetabolised  $^3\text{H}$ -P to tissue  $^3\text{H}$  content. The integral representing the area under the  $^3\text{H}$ -P curve was calculated using a trapezoidal approximation. An index of the tissue-specific rate of plasma FFA incorporation ( $R_{fs}$ ) was estimated as

$$R_{fs} = C_p \times K_{fs}$$

**Statistics.** Analyses of group data were based on four contrasts designed to specifically test the principle a priori questions of the study: LN versus OB (obesity effect), ROS1 versus OB, ROS10 versus OB, and DAR versus OB (treatment effects). Statistical significance of the contrasts were evaluated on the basis of  $F$  tests using the program SPSS (SPSS, Chicago, IL). Results are reported as means ± SE.  $P < 0.05$  was considered statistically significant.

## RESULTS

Body weights as well as plasma factors obtained via tail-vein blood sampling from 3-h fasted rats in the conscious state are presented in Table 1. Untreated obese Zucker rats were characterized by higher body weight, hyperglycemia, hyperinsulinemia, and hypertriglyceridemia compared with their age-matched lean controls. Thiazolidinedione treatment of the obese rats for 3 weeks resulted in significantly increased body weight gain. Estimates of lean and fat body masses (made using a whole-body conductivity method [14] in parallel identically treated series) indicate that a substantial component of the increased weight gain was a treatment-induced increase in fat body mass (Table 1). Thiazolidinediones very effectively lowered plasma glucose, insulin, and TG levels in the obese animals. Comparison of results for the two rosiglitazone-treated groups (ROS1 versus ROS10) indicated a consistent dose-dependent action on individual parameters. The two thiazolidinediones produced qualitatively similar effects, although darglitazone clearly had a

greater oral potency than rosiglitazone in this animal model, with darglitazone  $1.3 \mu\text{mol} \cdot \text{kg}^{-1} \cdot \text{day}^{-1}$  having similar effectiveness to rosiglitazone  $10 \mu\text{mol} \cdot \text{kg}^{-1} \cdot \text{day}^{-1}$ .

**Study 1: Plasma triglyceride kinetics and lipoprotein profiles.** Effects of Triton WR 1339 on plasma TG levels are presented in Fig. 1. In individual animals TG rose linearly with time (overall mean  $r^2 = 0.98$ ) irrespective of group, with no tendency to plateau over the 120-min post-Triton period. HTGO and  $K_{TG}$  are presented in Table 2. The substantial hypertriglyceridemia of the untreated obese Zucker rats was largely attributable to a greatly increased HTGO. There was also evidence that obese Zucker rats had an impaired capacity to clear plasma TG (Table 2). In the ROS1 group, plasma TG (obtained pre-Triton) was reduced compared with obese controls but remained elevated relative to the lean animals. This partial abolition of the hypertriglyceridemia was attributable to a selective increase in  $K_{TG}$ , with no effect on HTGO, as seen from the parallel TG accumulation curves for the obese control and ROS1 groups in Fig. 1. Darglitazone ( $1.3 \mu\text{mol} \cdot \text{kg}^{-1} \cdot \text{day}^{-1}$ ) and the higher dose of rosiglitazone (ROS10) reduced basal plasma TG toward the level of the lean group. This abolition of the hypertriglyceridemia was due to substantial increases in  $K_{TG}$  as well as marked reductions in the HTGO.

Lipoprotein profiles in plasma (Fig. 2) were assessed by on-line total cholesterol measurements of the elution profiles from the size exclusion chromatography column,

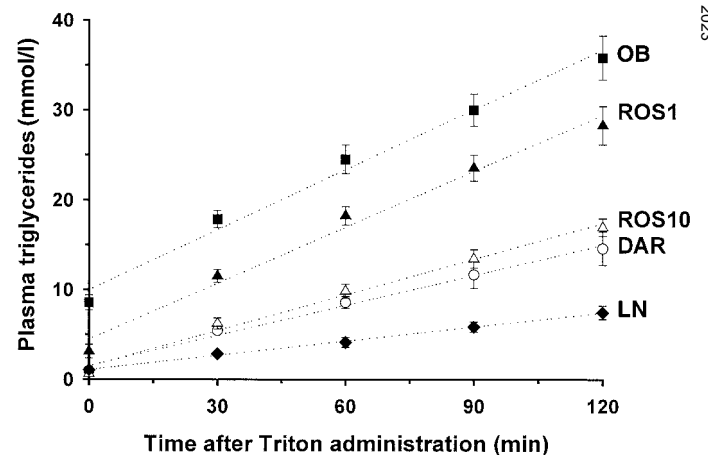


FIG. 1. Accumulation of plasma triglyceride in response to Triton WR 1339 administration in LN, OB, ROS1, ROS10, and DAR groups of Zucker rats. Results are expressed as means ± SE for  $n = 6-11$ .

TABLE 2

Hepatic production and whole-body clearance of plasma triglyceride and effects of obesity status and thiazolidinedione treatment

	LN	OB	ROS1	ROS10	DAR
Body weight (g)	400 ± 10*	618 ± 19	679 ± 15†	676 ± 13‡	704 ± 16*
Basal TG (mmol/l)	1.0 ± 0.2*	8.6 ± 0.9	3.1 ± 0.7*	0.6 ± 0.1*	0.9 ± 0.2*
Slope ( $\mu\text{mol} \cdot \text{ml}^{-1} \cdot \text{min}^{-1}$ )	0.053 ± 0.005*	0.222 ± 0.016	0.208 ± 0.015	0.133 ± 0.007*	0.112 ± 0.013*
$K_{TG}$ ( $\text{ml} \cdot \text{min}^{-1}$ )	0.85 ± 0.07	0.43 ± 0.06	1.42 ± 0.30†	3.88 ± 0.48*	2.13 ± 0.23*
HTGO rate ( $\mu\text{mol} \cdot \text{min}^{-1}$ )	0.8 ± 0.1*	3.3 ± 0.3	3.3 ± 0.2†	2.0 ± 0.1*	1.7 ± 0.2*

Data are means ± SE ( $n = 6-11$ ). Basal TG samples were collected just before Triton WR1339 administration. Slope (rate of increase of plasma TG), HTGO, and  $K_{TG}$  were calculated from the accumulation of TG in plasma following Triton WR 1339 administration. \* $P < 0.001$ , † $P < 0.01$ , ‡ $P < 0.05$  versus OB.

where the elution volume increases with decreasing lipoprotein particle size. This analysis was performed in all groups. Because the elution profiles were qualitatively similar in the thiazolidinedione-treatment groups, only results for the DAR and control groups are shown. Comparison of profiles from plasma samples obtained immediately before and 2 h after blockade of lipoprotein lipase action with Triton WR1339 enabled functional identification of the VLDL and lipoprotein remnant particles; VLDL is represented by the first eluted peak, which selectively increases during the post-Triton period because of ongoing VLDL secretion in the absence of VLDL elimination. The slower-eluting peaks represent lipoprotein remnants resulting from the catabolism and removal of TG from VLDL. These peaks are referred to as LDL and HDL, analogous with the lipoprotein profile in human plasma.

Comparison of the basal (pre-Triton) profiles indicates a substantial increase in VLDL particles in the plasma of obese untreated Zucker rats compared with lean animals. Treatment of the obese animals with thiazolidinediones virtually eliminated the VLDL peak while simultaneously

causing an increase in the abundance of the remnants: the area under the curves 40–60 min for DAR versus obese control rats was  $393 \pm 52$  vs.  $277 \pm 23$  mV/min,  $P < 0.05$ . These profile alterations are consistent with a thiazolidinedione-induced enhancement of VLDL-TG catabolism causing a redistribution of cholesterol from VLDL to smaller VLDL-remnant particles. Consistent with this mechanism, Triton administration to the darglitazone-treated animals reverted the profile to a pattern very similar to that of the untreated control animals (DAR post-Triton is compared with OB pre-Triton in Fig. 2).

#### Study 2: Mobilization and fate of plasma FFA.

**Whole-body FFA metabolism in anesthetized rats.** Whole-body FFA mobilization ( $R_a$ ) and  $K_p$  (an index of the combined ability of the body's tissues to take up FFA) were estimated based on steady-state tracer dilution using a constant infusion of  $\text{H}^3\text{H}$ -palmitate (Table 3). Obese untreated Zucker rats showed substantially elevated systemic FFA availability, with higher plasma FFA levels and  $R_a$  than the lean controls. Unexpectedly, thiazolidinedione treatment of the obese animals actually increased systemic FFA availability under fasting conditions with low insulin levels. Thus, in both the DAR and ROS10 groups,  $R_a$  was much higher (fourfold and 2.5-fold, respectively) than in the untreated controls. These large increases in  $R_a$  translated into relatively modest increments in plasma FFA due to large treatment-induced increases in  $K_p$  (DAR 2.4-fold and ROS10 twofold relative to untreated obese controls). Individual parameters in the ROS1 group did not achieve statistical significance; however, the means for  $R_a$ , plasma FFA, and  $K_p$  for this group lay between the corresponding means for the control and ROS10 groups, compatible with genuine effects at the lower dose.

**Whole-body and tissue-specific FFA metabolism in conscious rats.** Experiments were next performed in conscious animals to confirm the thiazolidinedione effects obtained in the anesthetized state. These much more detailed studies were limited to a comparison of obese untreated and DAR groups. To examine the effect of a physiological range of insulin levels on FFA metabolism, studies were conducted in both the basal fasting state and under conditions of the euglycemic-hyperinsulinemic clamp.

In the basal 7-h fasted state in conscious animals, darglitazone treatment approximately doubled both  $R_a$  (Fig. 3) and  $K_p$  (Table 4), qualitatively confirming the findings made in the anesthetized animals. In line with the results from the anesthetized animals, mean FFA levels tended to be higher with darglitazone treatment (Fig. 3), although this difference did not achieve statistical significance. Darglitazone treatment increased basal  $R_{ox}$  by 50%

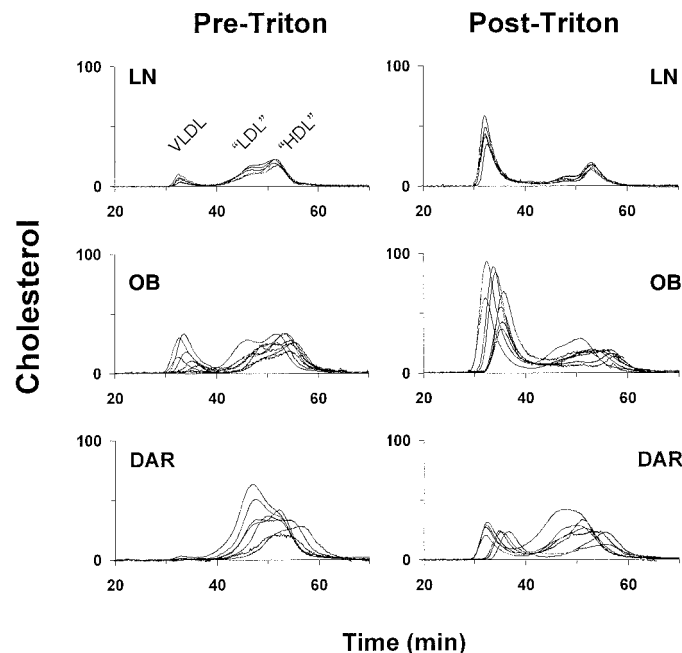


FIG. 2. Cholesterol distribution profiles in LN, OB, and DAR Zucker rats. Cholesterol concentration ( $y$ -axis), given in units of the spectrophotometer output mV, is plotted against elution time ( $x$ -axis). Profiles for each animal were obtained before (left hand panels) and 120 min (right hand panels) after Triton WR 1339 administration. Peaks have been labeled VLDL, LDL, and HDL analogous with the human lipoprotein profile.

TABLE 3

Whole-body FFA metabolism in 7-h fasted anesthetized Zucker rats and effects of obesity status and thiazolidinedione treatment

	LN	OB	ROS1	ROS10	DAR
Body weight (g)	380 ± 13*	634 ± 25	660 ± 14	754 ± 29*	778 ± 23*
Plasma FFA (mmol/l)	0.38 ± 0.03†	0.69 ± 0.06	0.79 ± 0.06	0.95 ± 0.08‡	1.15 ± 0.09*
$K_p$ (ml · min <sup>-1</sup> )	13.4 ± 0.9	20.8 ± 1.0	26.8 ± 3.5	42.0 ± 3.5*	50.6 ± 4.1*
$R_a$ (μmol · min <sup>-1</sup> )	5.2 ± 0.3‡	14.4 ± 1.3	20.9 ± 2.6	36.5 ± 1.8*	57.9 ± 6.0*

Data are means ± SE ( $n = 5$ ). \* $P < 0.001$ , † $P < 0.01$ , ‡ $P < 0.05$  versus OB.

(Fig. 3), although the treatment-induced increase in  $R_a$  was mostly directed into nonoxidative FFA metabolism ( $R_a - R_{ox}$  for DAR versus obese controls was  $45.5 \pm 4.6$  vs.  $19.4 \pm 1.9$  μmol · min<sup>-1</sup>,  $P < 0.001$ ). At the tissue level, darglitazone treatment induced a substantial elevation in the  $R_{fs}$  in adipose tissue in both BAT and WAT depots (Fig. 3). Darglitazone also induced a small increase in the  $R_{fs}$  of the glycolytic skeletal muscle WQ and tended to increase  $R_{fs}$  in RQ and liver. To exclude the influence of differences in FFA levels and isolate local tissue level effects,  $K_{fs}$  was calculated (Table 4). Of the various tissues examined, treatment only induced significant  $K_{fs}$  changes in adipose tissues.

To be able to perform the clamp studies at physiological levels of hyperinsulinemia, separate groups of control and darglitazone-treated obese animals were used to 1) measure postprandial plasma insulin levels in the freely fed state and 2) estimate the exogenous insulin infusion rates required to attain these postprandial insulin levels in 7-h fasted animals. From these extra studies, we estimated that the darglitazone-treated animals required only half the exogenous insulin infusion rate of the control animals ( $60$  vs.  $120$  pmol · kg<sup>-1</sup> lean body mass · min<sup>-1</sup>, respectively). Comparison of the plateau insulin levels achieved using these infusion rates (Table 5) with the fed insulin levels (DAR  $1.5 \pm 0.3$  nmol/l, obese control  $9.1 \pm 1.6$  nmol/l) confirmed that the clamps were performed at appropriate postprandial levels of hyperinsulinemia.

Darglitazone treatment markedly improved whole-body lipid- and glucose-metabolic insulin-mediated effects in the obese Zucker rats. Despite the much lower clamp insulin levels, DAR rats required a 2.8-fold higher glucose infusion rate (GIR) to maintain euglycemia compared with the untreated animals (Table 5). In response to the clamp, darglitazone treatment resulted in much greater suppression, leading to lower levels of plasma FFA as well as  $R_a$  and  $R_{ox}$  (Fig. 3). In DAR rats, there was a greater relative suppression of  $R_{ox}$  than  $R_a$  in response to the clamp. Thus, the ratio of  $R_{ox}$ -to- $R_a$  decreased from  $17 \pm 1\%$  in the basal state to  $11 \pm 1\%$  during the clamp in the treated animals ( $P < 0.01$ ), whereas in the untreated animals, no such reduction was observed (basal versus clamp:  $24 \pm 6$  vs.  $23 \pm 3\%$ ,  $P = 0.78$ ). During the clamp, darglitazone also reduced nonoxidative FFA disposal at the whole-body level ( $R_a - R_{ox}$ : DAR versus obese control,  $4.1 \pm 0.7$  vs.  $10.9 \pm 1.2$  μmol · min<sup>-1</sup>,  $P < 0.001$ ) and in all tissues examined (Fig. 3). Clamp adipose tissue  $K_{fs}$  results were generally very similar to the basal results, again showing the darglitazone-induced enhancement in the ability of adipose tissue to take up and store FFA (Table 4). In both DAR and untreated groups, skeletal muscle clamp  $K_{fs}$  was significantly higher than the basal  $K_{fs}$ . This insulin-mediated increase in muscle  $K_{fs}$  was larger in the darglitazone-

treated animals: the  $K_{fs}$  increased in WQ by 68% in DAR vs. 42% in control rats. Similarly, the  $K_{fs}$  increased in RQ by 91% in DAR vs. 32% in control rats.

**Hepatic triglyceride depots.** Liver weights and triglyceride contents are summarized in Table 6. Untreated obese Zucker rats had elevations in both liver weight and hepatic TG content (as compared with lean controls) that were partly reversed by thiazolidinedione treatment.

## DISCUSSION

The metabolic effects of the thiazolidinediones darglitazone and rosiglitazone on lipid metabolism as studied in obese *fafa* Zucker rats were qualitatively similar and are thus likely to be representative for this class of agents. Plasma TG lowering by thiazolidinediones was found to involve two kinetic mechanisms: decreased hepatic TG production and more rapid stripping of TG from VLDL particles. Furthermore, our detailed evaluation of their effects on FFA metabolism demonstrated that a major *in vivo* locus of thiazolidinedione action is in the adipose tissue, involving enhancements in both the capacity to liberate FFA under fasting conditions as well as insulin's ability to suppress FFA mobilization. These treatment effects in adipose tissue may provide metabolic flexibility by driving increased fatty acid utilization under fasting conditions and facilitating enhanced gluco-regulation under postprandial conditions.

Our results show that thiazolidinediones can eliminate

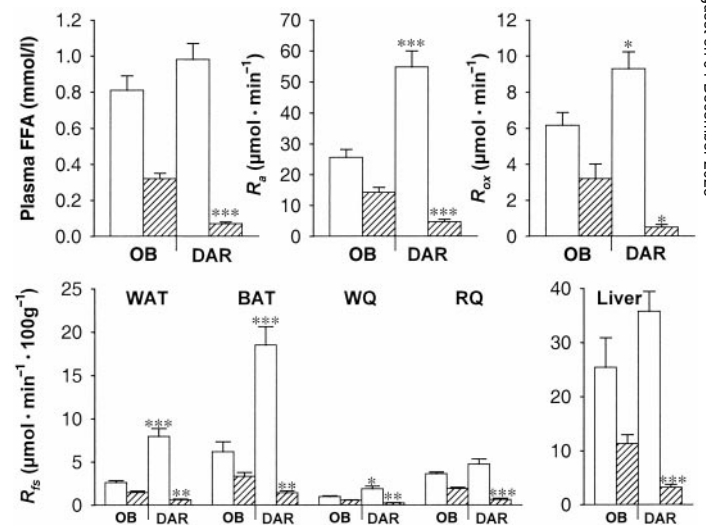


FIG. 3. Whole-body and tissue-specific FFA metabolism in OB or DAR obese Zucker rats. Results are expressed as means ± SE for  $n = 5$ . Animals were studied either in the basal fasting state (□) or during euglycemic clamps (▨). Whole-body parameters (plasma FFA,  $R_a$ , and  $R_{ox}$ ) are shown in the upper panels. Indexes of tissue-specific  $R_{fs}$  are shown in the lower panels. \* $P < 0.05$ ; \*\* $P < 0.01$ ; \*\*\* $P < 0.001$  vs. OB rats.

TABLE 4

Whole-body and tissue-specific (nonoxidative) clearance of plasma FFA in conscious 7-h fasted obese Zucker rats and effects of darglitazone

	OB		DAR	
	Basal	Clamp	Basal	Clamp
Body weight (g)	541 ± 10	629 ± 25	670 ± 26*	684 ± 22
$K_p$ (ml · min <sup>-1</sup> )	30.8 ± 0.9	44.0 ± 3.3§	55.5 ± 4.0†	64.8 ± 5.9‡
Tissue $K_{fs}$ (ml · 100 g <sup>-1</sup> · min <sup>-1</sup> )				
WAT	3.2 ± 0.3	4.3 ± 0.5	7.4 ± 1.1*	8.6 ± 0.9*
BAT	7.3 ± 1.0	9.9 ± 0.7	17.6 ± 2.0†	20.6 ± 3.2*
WQ	1.2 ± 0.1	1.7 ± 0.1§	1.9 ± 0.3	3.2 ± 0.4  *
RQ	4.4 ± 0.3	5.8 ± 0.5	4.7 ± 0.4	8.7 ± 1.5
Liver	30.3 ± 4.6	34.9 ± 4.5	35.9 ± 1.3	45.8 ± 5.8

Data are means ± SE ( $n = 5$ ). \* $P < 0.001$ , † $P < 0.01$ , ‡ $P < 0.05$  versus OB in same state (either clamp or basal). § $P < 0.01$ , || $P < 0.05$ , fasted versus clamped in same group (either OB or DAR).

the extreme hypertriglyceridemia of the obese Zucker rat. One component of this antihypertriglyceridemic action was increased plasma TG clearance. An accelerated conversion of VLDL to triglyceride-poor remnants lowered VLDL and raised remnant concentrations in the plasma. This mode of thiazolidinedione action has previously been indicated in experiments in normal animals (15). The present study extends those observations by examination of a dyslipidemic animal model using an informative experimental paradigm (the combined use of Triton WR 1339 and lipoprotein analysis) that enabled functional identification of the VLDL and remnant lipoprotein fractions.

In addition to the treatment-induced enhancement of plasma TG clearance, the thiazolidinediones also lowered plasma TG levels by reducing the rate of HTGO. A higher dose requirement for the HTGO-lowering action than for the plasma TG clearance-enhancing mechanism was indicated in a comparison of the effects of the two rosiglitazone doses (Table 2) and may explain apparent discrepancies regarding kinetic mechanisms of TG lowering by different members of this group of agents. Thus, studies demonstrating effects only on clearance (13–17) may have examined responses to effectively lower doses than those used in the current study and in another study (2). The HTGO-lowering action was associated with (and may have been at least partly mediated by) treatment-induced reductions in intrahepatic hepatic TG stores (Table 6), an important source of lipids for VLDL assembly (18).

To elucidate the effects of thiazolidinediones on the kinetic processes that determine plasma FFA levels over a physiological range of insulin levels, studies were conducted in both the basal 7-h fasted state and during euglycemic

clamps (performed at insulin levels corresponding to those observed postprandially). Increased plasma FFA clearance was a robust thiazolidinedione action observed in both the basal and clamp situations. In contrast, the effects of thiazolidinediones on  $R_a$  were totally opposite in basal and clamp states. In the basal state, there was a substantial increase in  $R_a$ . Although initially surprising, this effect was considered consistent with the actions of the thiazolidinediones to induce adipocyte proliferation (19) and upregulate adipose tissue genes involved in FFA exchange with plasma (10,20). At the low fasting insulin levels in the treated animals, these actions may have provided the molecular machinery for this enhanced  $R_a$ .

Whatever the mechanism, the increase in  $R_a$  was sufficient to cancel out the influence of enhanced FFA clearance. In fact, fasting FFA levels tended to be higher in the treated animals. Under clamp conditions, treatment resulted in substantially lower plasma FFA levels because of the combined effects of much greater suppression of  $R_a$  (a manifestation of insulin sensitization in adipose tissue) and the increase in FFA clearance. Altogether, the results of the clamp and basal studies showed that thiazolidinediones induced a substantially larger change in plasma FFA levels across a physiological range of insulin levels. This implies more rapid and larger changes in FFA levels in the transition from the fed state to fasting. There is a practical implication of this situation on the assessment of thiazolidinedione effects on FFA levels. In fed animals, FFA levels are expected to be consistently lower, but as the length of fasting increases after food withdrawal, this treatment effect may become nonapparent or even reversed.

We propose that the actions of thiazolidinediones on adipose tissue FFA release provide a basis for more widespread tissue effects that lead to an improvement in whole-body metabolic flexibility, as evidenced by increased fatty acid oxidation under fasting conditions and improved glucohomeostasis under hyperinsulinemic conditions. Therefore, the augmented FFA mobilization may drive the enhanced whole-body FFA oxidation in the fasting state. We did not assess peripheral glucose utilization, but based on the reciprocal relationship between glucose and fatty acid catabolism (21), the elevation of FFA oxidation under fasting conditions may well be accompanied by a reduction in glucose oxidation. Under conditions of insulin stimulation, the much more effective

TABLE 5

Responses to glucose clamps and whole-body insulin-stimulated glucose metabolism in conscious obese Zucker rats and effects of darglitazone

	OB	DAR
Preclamp state		
Blood glucose (mmol/l)	4.9 ± 0.2	4.6 ± 0.2
Plasma insulin (nmol/l)	3.6 ± 0.8	0.43 ± 0.1*
Clamped state		
Blood glucose (mmol/l)	5.2 ± 0.2	4.7 ± 0.2
Plasma insulin (nmol/l)	9.6 ± 1.1	1.8 ± 0.04†
GIR (mg · min <sup>-1</sup> )	4.7 ± 0.5	13.3 ± 0.9†

Data are means ± SE ( $n = 5$ ). \* $P < 0.01$ , † $P < 0.001$  versus OB.

TABLE 6  
Liver weight and triglyceride content

	LN	OB	ROS1	ROS10	DAR
Liver weight (g)	10.1 ± 0.2*	26.9 ± 1.4	22.5 ± 1.1†	18.3 ± 0.9*	20.3 ± 1.5*
Liver TG (g · 100g <sup>-1</sup> )	2.5 ± 0.3*	14.8 ± 1.4	12.7 ± 0.8	13.5 ± 2.3	5.5 ± 0.5*
Total liver TG (g)	0.25 ± 0.03*	4.01 ± 0.47	2.87 ± 0.25‡	2.55 ± 0.51†	1.13 ± 0.15*

Data are means ± SE ( $n = 6-11$ ). \* $P < 0.001$ , † $P < 0.01$ , ‡ $P < 0.05$  versus OB.

suppression of FFA mobilization possibly plays an important indirect role in the observed improvements in whole-body glucoregulation. Decreased fatty acid availability and oxidation could theoretically increase both glucose utilization in skeletal muscle and insulin suppression of hepatic glucose production (HGP) (22). Tissue-specific glucose metabolism was not assessed in the current study. However, previous studies of thiazolidinediones have clearly established that major components of the whole-body insulin sensitization are increased insulin-stimulated muscle glucose utilization (23–26) and an enhanced ability of insulin to suppress HGP (24,27).

Thiazolidinedione treatment enhanced the ability of adipose tissue to take up and store FFA (Table 4). This enhanced ability allied with the large adipose tissue mass of the obese Zucker rats increased plasma FFA clearance. Figure 4 represents a breakdown of the tissue distribution and fate of plasma FFA calculated from the whole-body and tissue-specific flux determinations (Fig. 3) as well as estimates of tissue weights. Darglitazone treatment in both the basal fasting and clamp situations thus resulted in much greater trafficking of FFA into adipose tissues and away from oxidative metabolism as well as greater non-oxidative disposal in the liver. Adding together the estimated contributions of whole-body oxidative disposal ( $R_{ox}$ ) and nonoxidative disposal in skeletal muscles, liver, and white adipose tissue, we were able to account for >79% of the FFA leaving the plasma in all groups. Non-oxidative disposal into other tissues (including those not examined at all and BAT, whose tissue mass is unknown) make up the remaining fraction of whole-body FFA disposal. The current demonstration that thiazolidinediones enhance FFA uptake by adipose tissue fits well with reports that PPAR $\gamma$  agonists upregulate adipose tissue gene expression of molecules involved in FFA transport and metabolism, including a putative fatty acid transporter protein, fatty acid translocase, and acyl-CoA synthetase (10,20). To our knowledge, the present data provide the first in vivo evidence that these changes in gene expression are of functional significance for FFA metabolism.

Most, but not all, of the actions of thiazolidinediones on FFA metabolism could be considered a direct result of their effects in adipose tissue. Darglitazone enhanced the insulin-mediated suppression of FFA oxidation not just indirectly via greater suppression of FFA mobilization but also (as seen in Fig. 4) by decreasing the fraction of FFA undergoing oxidative metabolism. Our data indicate that skeletal muscle was responsible for this whole-body effect. Thus, the analysis in Fig. 4 shows that the insulin-mediated decrease in the FFA oxidation fraction was quantitatively matched by a corresponding increase in the fractional nonoxidative disposal into muscle. Treatment may thus induce a greater shift in the metabolic fate of FFA taken up

by muscle, from oxidative metabolism under fasting conditions to nonoxidative disposal under hyperinsulinemic conditions. The mechanism of this effect remains to be clarified, although inhibition of FFA entry into mitochondria (28) and increased FFA esterification (29) are possible alternatives.

In conclusion, thiazolidinediones induced remarkable changes in the handling and fate of lipids in the obese Zucker rat. The results point to a critical role of adipose tissue FFA metabolism in both the general metabolic dysregulation of the obese animals and the subsequent thiazolidinedione-induced amelioration of this condition. The present data indicate that treatment with thiazolidinediones allows much greater metabolic flexibility to utilize lipids and carbohydrates in the fasting and postprandial states, respectively. In addition, we have shown that thiazolidinedione-induced abolition of hypertriglyceridemia in this model was attributable to the combination of enhanced VLDL-TG catabolism and reduced hepatic TG secretion.

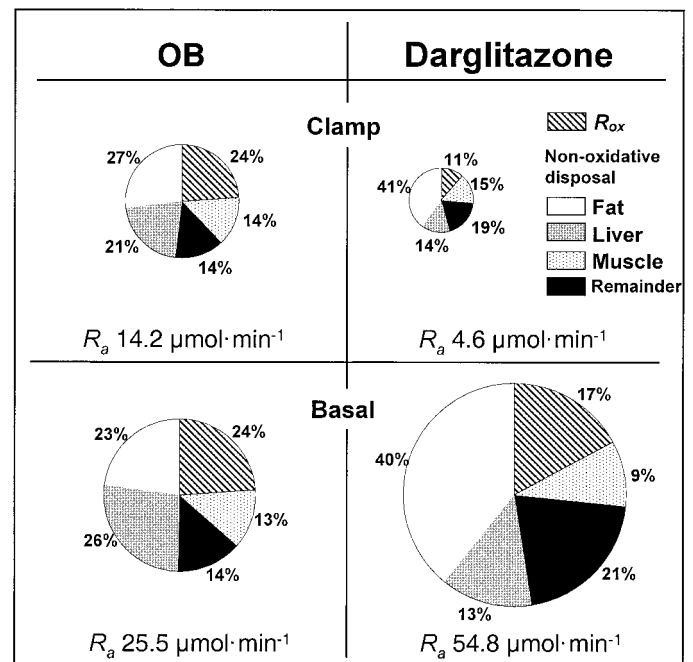


FIG. 4. Mobilization and fate of plasma FFA in OB and DAR obese 7-h fasted Zucker rats. Studies were conducted either during a glucose clamp (upper panels) or in the basal state (lower panels). The total area of each pie diagram is proportional to the whole-body  $R_a$ . Component fractions represent whole-body  $R_{ox}$  and indexes of nonoxidative FFA disposal in muscle, liver, and white adipose tissue calculated from  $R_{fs}$  data (muscle = average of WQ and RQ) and tissue weights obtained from weighing (liver), body composition analysis (adipose tissue), and (30) (muscle). The fraction of  $R_a$  not accounted for (remainder) is directed to nonoxidative FFA disposal in unmeasured tissues and BAT.

## ACKNOWLEDGMENTS

We are grateful to Germán Camejo for his valuable input and for reviewing the manuscript. We also thank Lennart Svensson and his group for performing the biochemical analyses and particularly for the effort to produce the lipoprotein profile analysis.

## REFERENCES

- Chang AY, Wyse BM, Gilchrist BJ, Peterson T, Diani AR: Ciglitazone, a new hypoglycemic agent. I. Studies in *ob/ob* and *db/db* mice, diabetic Chinese hamsters, and normal and streptozotocin-diabetic rats. *Diabetes* 32:830–838, 1983
- Fujiwara T, Yoshioka S, Yoshioka T, Ushiyama I, Horikoshi H: Characterization of new oral antidiabetic agent CS-045: studies in KK and *ob/ob* mice and Zucker fatty rats. *Diabetes* 37:1549–1558, 1988
- Ikeda H, Taketomi S, Sugiyama Y, Shimura Y, Sohda T, Meguro K, Fujita T: Effects of pioglitazone on glucose and lipid metabolism in normal and insulin resistant animals. *Arzneimittelforschung* 40:156–162, 1990
- Young PW, Cawthorne MA, Coyle PJ, Holder JC, Holman GD, Kozka IJ, Kirkham DM, Lister CA, Smith SA: Repeat treatment of obese mice with BRL 49653, a new potent insulin sensitizer, enhances insulin action in white adipocytes: association with increased insulin binding and cell-surface GLUT4 as measured by photoaffinity labeling. *Diabetes* 44:1087–1092, 1995
- Sohda T, Mizuno K, Imamiya E, Sugiyama Y, Fujita T, Kawamatsu Y: Studies on antidiabetic agents. II. Synthesis of 5-[4-(1-methylcyclohexylmethoxy)-benzyl]thiazolidine-2,4-dione (ADD-3878) and its derivatives. *Chem Pharm Bull (Tokyo)* 30:3580–3600, 1982
- Boden G: Free fatty acids, insulin resistance, and type 2 diabetes mellitus (Review). *Proc Assoc Am Physicians* 111:241–248, 1999
- Lehmann JM, Moore LB, Smith-Oliver TA, Wilkison WO, Willson TM, Kliewer SA: An antidiabetic thiazolidinedione is a high affinity ligand for peroxisome proliferator-activated receptor gamma (PPAR $\gamma$ ). *J Biol Chem* 270:12953–12956, 1995
- Braissant O, Foufelle F, Scotto C, Dauca M, Wahli W: Differential expression of peroxisome proliferator-activated receptors (PPARs): tissue distribution of PPAR- $\alpha$ , - $\beta$ , and - $\gamma$  in the adult rat. *Endocrinology* 137:354–366, 1996
- Schoonjans K, Staels B, Auwerx J: The peroxisome proliferator activated receptors (PPARs) and their effects on lipid metabolism and adipocyte differentiation. *Biochim Biophys Acta* 1302:93–109, 1996
- Martin G, Schoonjans K, Lefebvre AM, Staels B, Auwerx J: Coordinate regulation of the expression of the fatty acid transport protein and acyl-CoA synthetase genes by PPAR $\alpha$  and PPAR $\gamma$  activators. *J Biol Chem* 272:28210–28217, 1997
- Hagenfeldt L: A gas chromatographic method for the determination of individual free fatty acids in plasma. *Clinica Chimica Acta* 13:266–268, 1966
- Sartipy P, Camejo G, Svensson L, Hurt-Camejo E: Phospholipase A(2) modification of low density lipoproteins forms small high density particles with increased affinity for proteoglycans and glycosaminoglycans. *J Biol Chem* 274:25913–25920, 1999
- Otway S, Robinson DS: The use of a non-ionic detergent (Triton WR 1339) to determine rates of triglyceride entry into the circulation of the rat under different physiological conditions. *J Physiol* 190:321–332, 1967
- Bracco EF, Yang MU, Segal K, Hashim SA, Van Itallie TB: A new method for estimation of body composition in the live rat. *Proc Soc Exp Biol Med* 174:143–146, 1983
- Lefebvre AM, Peinado-Onsurbe J, Leitersdorf I, Briggs MR, Paterniti JR, Fruchart JC, Fievet C, Auwerx J, Staels B: Regulation of lipoprotein metabolism by thiazolidinediones occurs through a distinct but complementary mechanism relative to fibrates. *Arterioscler Thromb Vasc Biol* 17:1756–1764, 1997
- Fujita T, Sugiyama Y, Taketomi S, Sohda T, Kawamatsu Y, Iwatsuka H, Suzuoki Z: Reduction of insulin resistance in obese and/or diabetic animals by 5-[4-(1-methylcyclohexylmethoxy)benzyl]-thiazolidine-2,4-dione (ADD-3878, U-63,287, ciglitazone), a new antidiabetic agent. *Diabetes* 32:804–810, 1983
- Kaumi T, Hirano T, Odaka H, Ebara T, Amano N, Hozumi T, Ishida Y, Yoshino G: VLDL triglyceride kinetics in Wistar fatty rats, an animal model of NIDDM: effects of dietary fructose alone or in combination with pioglitazone. *Diabetes* 45:806–811, 1996
- Gibbons GF, Bartlett SM, Sparks CE, Sparks JD: Extracellular fatty acids are not utilized directly for the synthesis of very-low-density lipoprotein in primary cultures of rat hepatocytes. *Biochem J* 287:749–753, 1992
- Okuno A, Tamemoto H, Tobe K, Ueki K, Mori Y, Iwamoto K, Umesono K, Akanuma Y, Fujiwara T, Horikoshi H, Yazaki Y, Kadowaki T: Troglitazone increases the number of small adipocytes without the change of white adipose tissue mass in obese Zucker rats. *J Clin Invest* 101:1354–1361, 1998
- Motojima K, Passilly P, Peters JM, Gonzalez FJ, Latruffe N: Expression of putative fatty acid transporter genes are regulated by peroxisome proliferator-activated receptor  $\alpha$  and  $\gamma$  activators in a tissue- and inducer-specific manner. *J Biol Chem* 273:16710–16714, 1998
- Randle PJ, Garland PB, Hales CN, Newsholme EA: The glucose-fatty acid cycle: its role in insulin sensitivity and metabolic disturbances of diabetes mellitus. *Lancet* 1:785–794, 1963
- Rebrin K, Steil GM, Getty L, Bergman RN: Free fatty acid as a link in the regulation of hepatic glucose output by peripheral insulin. *Diabetes* 44:1038–1045, 1995
- Kraegen EW, James DE, Jenkins AB, Chisholm DJ, Storlien LH: A potent in vivo effect of ciglitazone on muscle insulin resistance induced by high fat feeding of rats. *Metabolism* 38:1089–1093, 1989
- Oakes ND, Kennedy CJ, Jenkins AB, Laybutt DR, Chisholm DJ, Kraegen EW: A new antidiabetic agent, BRL 49653, reduces lipid availability and improves insulin action and glucoregulation in the rat. *Diabetes* 43:1203–1210, 1994
- Zierath JR, Ryder JW, Doebber T, Woods J, Wu M, Ventre J, Li Z, McCrory C, Berger J, Zhang B, Moller DE: Role of skeletal muscle in thiazolidinedione insulin sensitizer (PPAR $\gamma$  agonist) action. *Endocrinology* 139:5034–5041, 1998
- Hallakou S, Foufelle F, Doare L, Kergoat M, Ferre P: Pioglitazone-induced increase of insulin sensitivity in the muscles of the obese Zucker *fa/fa* rat cannot be explained by local adipocyte differentiation. *Diabetologia* 41:963–968, 1998
- Sugiyama Y, Shimura Y, Ikeda H: Effects of pioglitazone on hepatic and peripheral insulin resistance in Wistar fatty rats. *Arzneimittelforschung* 40:436–440, 1990
- Sidossis LS, Stuart CA, Shulman GI, Lopaschuk GD, Wolfe RR: Glucose plus insulin regulate fat oxidation by controlling the rate of fatty acid entry into the mitochondria. *J Clin Invest* 98:2244–2250, 1996
- Sul HS, Wang D: Nutritional and hormonal regulation of enzymes in fat synthesis: studies of fatty acid synthase and mitochondrial glycerol-3-phosphate acyltransferase gene transcription. *Ann Rev Nutr* 18:331–351, 1998
- Hom FG, Goodner CJ, Berrie MA: A [ $^3$ H]-2-deoxyglucose method for comparing rates of glucose metabolism and insulin responses among rat tissues in vivo: validation of the model and the absence of an insulin effect on brain. *Diabetes* 33:141–152, 1984